



Title	Corrosion Mechanism of Silver Brazed Stainless Steel Joint in Chloride Solutions(Materials, Metallurgy, Weldability)
Author(s)	Okamoto, Ikuo; Takemoto, Tadashi
Citation	Transactions of JWRI. 1980, 9(2), p. 217-223
Version Type	VoR
URL	<a href="https://doi.org/10.18910/4940">https://doi.org/10.18910/4940</a>
rights	
Note	

*The University of Osaka Institutional Knowledge Archive : OUKA*

<https://ir.library.osaka-u.ac.jp/>

The University of Osaka

# Corrosion Mechanism of Silver Brazed Stainless Steel Joint in Chloride Solutions<sup>†</sup>

Ikkuo OKAMOTO\* and Tadashi TAKEMOTO\*\*

## Abstract

*Electrochemical and metallographic studies have been made on the silver brazed SUS 304 stainless steel joint to demonstrate the interfacial corrosion mechanisms in sodium chloride solutions with additions of cupric chloride. The corrosion behaviours of silver brazed stainless steel joints have been investigated as functions of pH, cupric chloride concentration and composition of filler alloy. Polarization measurements revealed that the removal of corrosion resistant passive films on stainless steel by brazing flux during brazing was one of the causes of interfacial corrosion of stainless steel at brazed interface. Formation of nickel depleted zone in SUS 304 at brazing interface also appeared to be responsible to the cause of interfacial corrosion.*

*The added copper to corrosive solution enhanced the cathodic reaction of both stainless steel at brazed interface and filler alloy. As a result of cathodic reduction, metallic copper precipitated on cathodes such as  $\alpha_1$ -Ag phase of filler alloy and bulk stainless steel surface. Preferential dissolved zinc and copper from  $\alpha$ -Cu phase adhered as chlorides to specimen surface. The pH change of corrosive solution during immersion test appeared to be caused by precipitation of added copper, dissolution of iron, zinc and other alloying elements.*

**KEY WORDS:** (Corrosion) (Brazed Joints) (Filler Materials) (Austenitic Stainless Steels) (Halides)

## 1. Introduction

The corrosion resistance of silver brazed stainless steel joints is sometimes not so satisfactory in the aqueous solutions containing chlorides. The evaluation methods for the corrosion resistance of brazed joint have not been established yet, however, the observation of appearance, the measurement of weight loss, the decrement of tensile strength and corrosion depth have been adopted<sup>1)–3)</sup>. But there is no satisfying correlations between weight loss and the decrease in tensile strength<sup>1)</sup>. This may be caused by the differences in corrosion characteristics and formation of voids and intermetallic compounds at brazed interface. The authors<sup>4)</sup> designed a new shape specimen for evaluation of the corrosion of brazed joint, and observed the corrosion characteristics of silver brazed joint. The new specimen made it possible to evaluate the simultaneous corrosion of brazed filler alloy itself and the interfacial corrosion at brazed part respectively. This investigation was concerned with the mechanism of corrosion at interface between silver filler alloy and stainless steel brazed joint in chloride solutions.

## 2. Experimental Procedures

Figure 1 shows the shape and size of the new type specimen with a brazed groove. The nominal chemical compositions of filler alloys are shown in Table 1, and the used base material is SUS 304 stainless steel. Corrosion test were carried out in 0.4 mol/l NaCl aqueous solutions containing 0 ~ 0.05 mol/l CuCl<sub>2</sub> (Table 2) by the immersion of specimen for predetermined periods. Test temperature was maintained at 25°C by a thermostat.

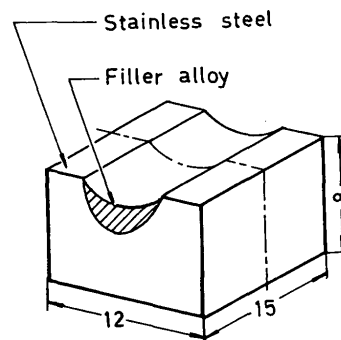


Fig. 1 Shape and size of specimen

<sup>†</sup> Received on September 24, 1980

\* Professor

\*\* Research Instructor

**Table 1** Nominal chemical compositions of filler alloys (wt%)

Filler alloys	Ag	Cu	Zn	Cd	Ni	Brazing temp. (°C)
BAg-1a	50	15.5	16.5	18	-	710
BAg-3	50	15.5	15.5	16	3	770
BAg-4	40	30	28	-	2	830
BAg-5	45	30	25	-	-	795

**Table 2** Chemical compositions of corrosive solutions (mol/l)

Solutions	NaCl	CuCl <sub>2</sub> ·2H <sub>2</sub> O
A-1	0.4	0.0
B-1	0.4	0.0005
B-2	0.4	0.005
B-3	0.4	0.05

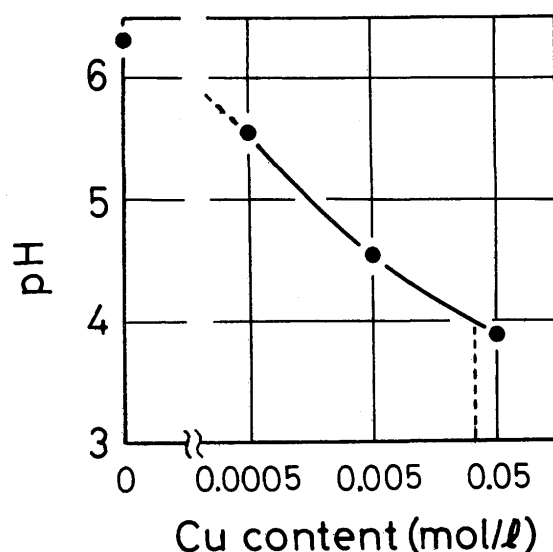
Precise experimental techniques were described in previous paper<sup>4)</sup>. The corrosion profile was observed by optical and scanning electron microscopes. The change of pH of corrosive solution during corrosion test was measured by pH meter.

### 3. Results

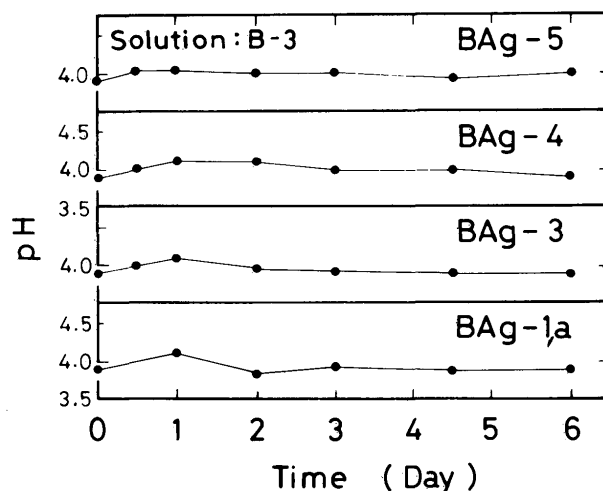
#### 3.1 Characteristics of Corrosive Solutions

Figure 2 shows the change of pH of corrosive solution by the addition of cupric chloride. The pH of A-1 solution without copper addition was 6.3, and it decreased with the increase in cupric chloride content, the pH of solution with 0.05 mol/l cupric chloride decreased to 3.9. The chloride content also increased by addition of cupric chloride, however, the pH of 1.0 mol/l NaCl solution without copper was 5.9. As B-3 solution contained 0.5 mol/l chlorine, the decrease in pH by the addition of cupric chloride mainly related to the increase in copper concentration in corrosive solutions and was not caused by the increase in chlorine ion. The added copper is stable as Cu<sup>2+</sup> cupric ion and exhibits light blue color in the pH range shown in Fig. 2.

Figure 3 shows the changes of pH during corrosion test on the specimen brazed with various filler alloys. The pH slightly increased after immersion for 0.5 ~ 1 day and then settled about 4. The slight increase in pH during initial period of immersion was due to the precipitation of copper dissolved in corrosive solution by cathodic reaction. Figure 4 shows the precipitated copper on the filler alloy at the interface of filler alloy and base metal. The



**Fig. 2** Relation between pH and copper content in 0.4 mol/l NaCl solutions, dotted line shows the change of pH by decrease of 0.016 mol/l cupric chloride from B-3 solution



**Fig. 3** Changes of pH of corrosive solutions during immersion tests in B-3 solution

precipitated particle size and the amount might be dependent on the weight loss and immersion time, the particle size shown in Fig. 4 was almost under 40 μ in diameter.

Chemical analysis of B-3 corrosive solutions revealed that precipitated copper was about 1000 ppm after corrosion test for 4.5 days. One thousand ppm of copper corresponds 0.016 mol/l, therefore, as shown in Fig. 2 by dotted lines, pH rised to 4.0 with decreasing 0.016 mol/l copper in B-3 solution. This coincided well with the observed pH of more than 2 days as shown in Fig. 3,

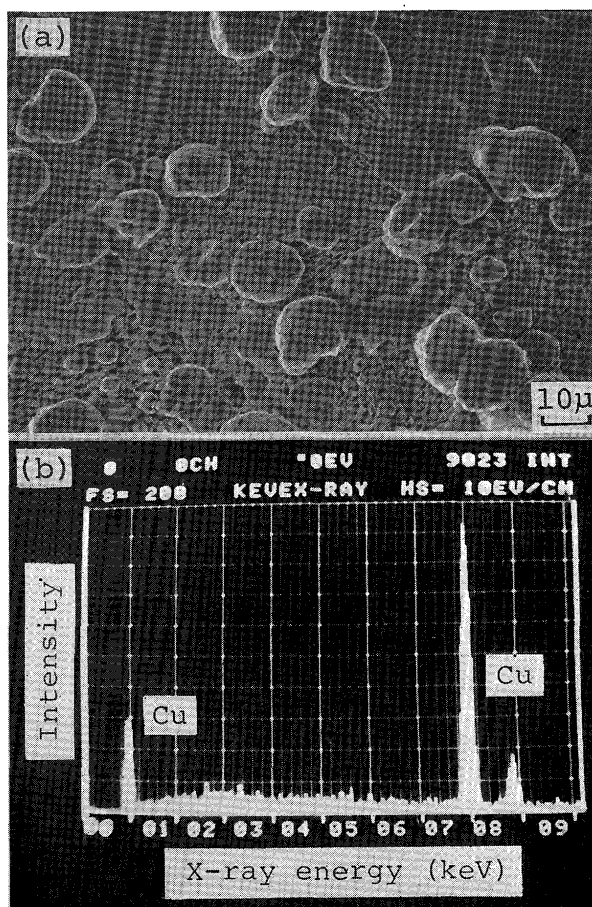


Fig. 4 Scanning electron micrograph of deposited copper on BAg-3 (a) and energy dispersive analysis of deposited copper (b)

however, the pH once increased to 4.1 at the first stage of immersion ( $\sim 1$  day) and then gradually decreased. Thus the changes of pH during immersion test of silver brazed specimens were seemed to depend not only on the precipitation of copper but also on the dissolution of iron, zinc and other constituents. The immersion time dependences of corrosion depth of filler alloy and interfacial corrosion length were measured, and the results showed well known parabolic law, whereas the pH did not changed as parabola, showing that there was no significant relations between pH change and corrosion rate.

### 3.2 Effect of Copper Concentration on Corrosion

As mentioned in previous paper, two types of corrosion, the corrosion of filler alloy itself and the interfacial corrosion at interface between filler alloy and stainless steel, simultaneously proceeded. The corrosion of filler alloy was preferential dissolution of  $\alpha$ -Cu phase (mainly consisted of Cu-Zn solid solution). The corrosion depth

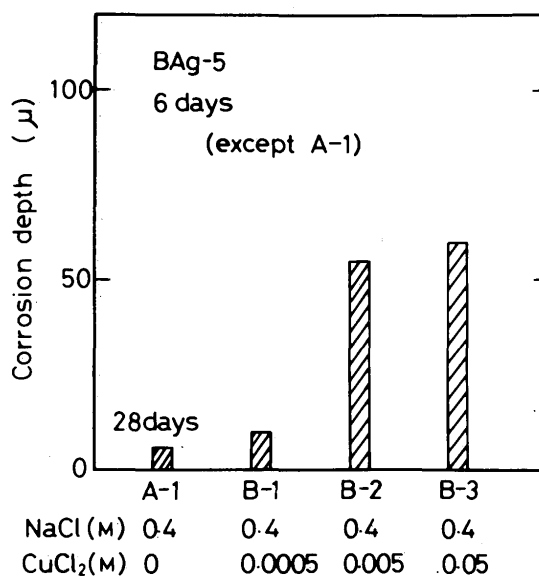


Fig. 5 Effect of copper content on the corrosion depth of filler alloy (BAg-5)

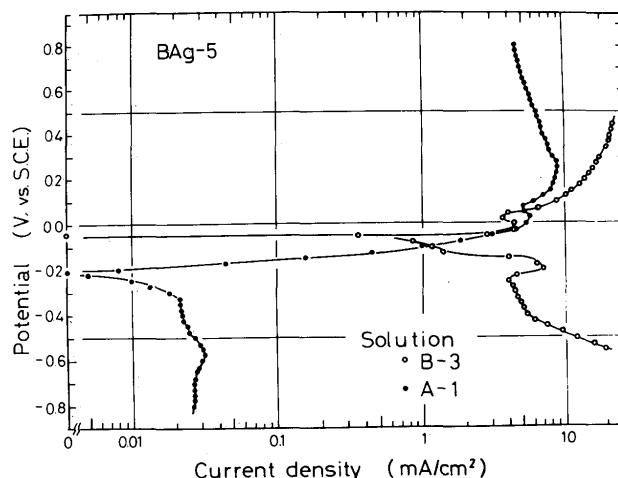


Fig. 6 Anodic and cathodic polarization curves of BAg-5 in A-1 and B-3 solutions

from filler alloy surface in chloride solutions with various copper content is shown in Fig. 5. The corrosion depth in A-1 solution without copper addition was about  $6 \mu$  after 28 day immersion, but it was  $10 \mu$  in the solution of  $0.0005 \text{ mol/l}$  copper, and was about  $60 \mu$  in the solution of more than  $0.05 \text{ mol/l}$  copper. The copper addition in NaCl aqueous solution enhanced the corrosion of filler alloy.

Figure 6 shows the anodic and cathodic polarization curves of brazed BAg-5 filler alloy in A-1 and B-3 solutions. The addition of copper in solution did not give large differences to the anodic polarization curves, but it

enhanced the cathodic reaction and consequently increased the limiting current density<sup>5)</sup>. The accelerated corrosion in solutions containing copper resulted in the enhanced cathodic reaction in these corrosive solutions. The natural electrode potential of brazed specimen in A-1 and B-3 solutions were about  $-250$  mV (S.C.E.) and  $-50$  mV respectively and the values showed no great change during immersion test. No marked differences in natural electrode potentials of brazed specimens were found irrespective of the composition of brazing filler alloys. This appears to be due to the surface area ratio of filler alloy to stainless steel was about 1 : 8, and moreover, the electrode potentials of silver filler alloys and stainless steel were not so different from each other.

### 3.3 Morphology of Corrosion

Figure 7 shows the surface of the brazed filler alloys after immersion in B-3 solution for 3 days. The surface was rinsed in ultrasonic water bath and acetone bath prior to observation. Preferential dissolution of dendritic  $\alpha$ -Cu phase is shown. The results of energy dispersive analysis of the surface showed that zinc and chlorine mainly existed.

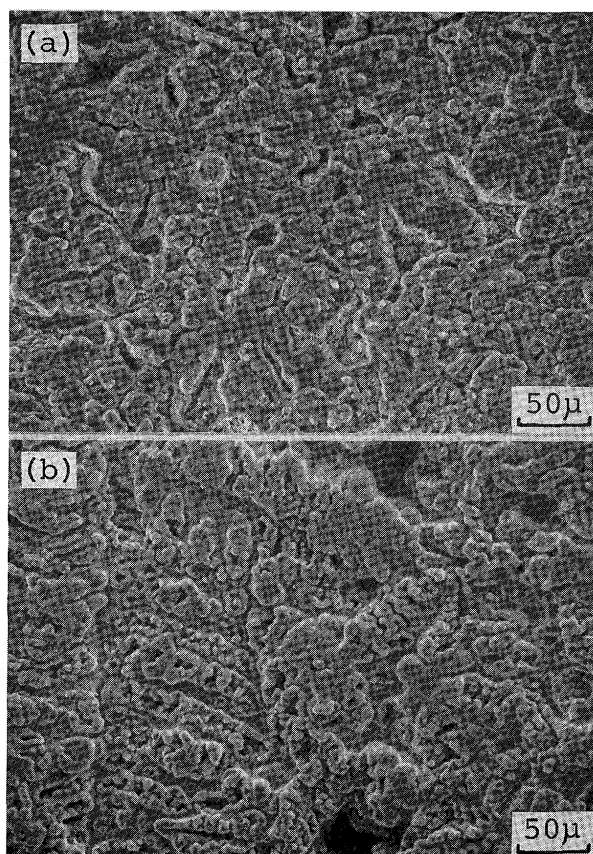


Fig. 7 Scanning electron micrographs of surface of BAg-5 (a) and BAg-4 (b) after corrosion in B-3 for 3 days

X-ray diffraction analysis on the corrosion products attached to the specimen surface proved the existence of CuCl, and other many diffraction lines were observed, however, they could not be solved.

Figure 8 (a) shows the penetrated corrosion tips at interface between filler alloy and stainless steel. Brazed filler alloy was peeled off by force from base metal in order to observe the tip of interfacial corrosion. Plastic deformation of filler alloy and uniform general corrosion of stainless steel are presented, but the unevenness of surface of corroded stainless steel became rough with the progress of corrosion (Fig. 8 (b)). Precipitated copper was not observed on the surface of stainless steel at brazed interface.

Figure 9 shows the precipitated copper on the filler alloy at brazed interface (a) and at surface (b) of the silver brazed stainless steel specimen after corrosion test. From Fig. 4, 8 and 9, copper precipitated mainly on the filler alloy. Consequently, the cathodic site is seemed to exist in filler alloy, and the stainless steel at brazed interface dissolves anodically by the local corrosion cell between silver filler alloy and neighbouring stainless steel. The corrosion of silver filler alloy, consisted of  $\alpha$ -Cu phase and  $\alpha_1$ -Ag phase, proceeded by the preferential dissolution of  $\alpha$ -Cu

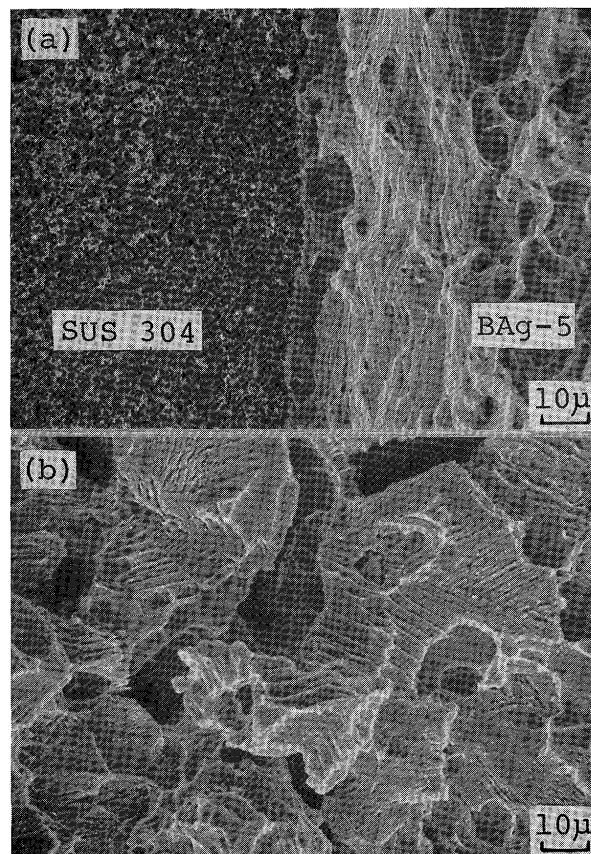


Fig. 8 Penetrated corrosion tip (a) and corroded SUS 304 (b) after corrosion in B-3 for 3 days

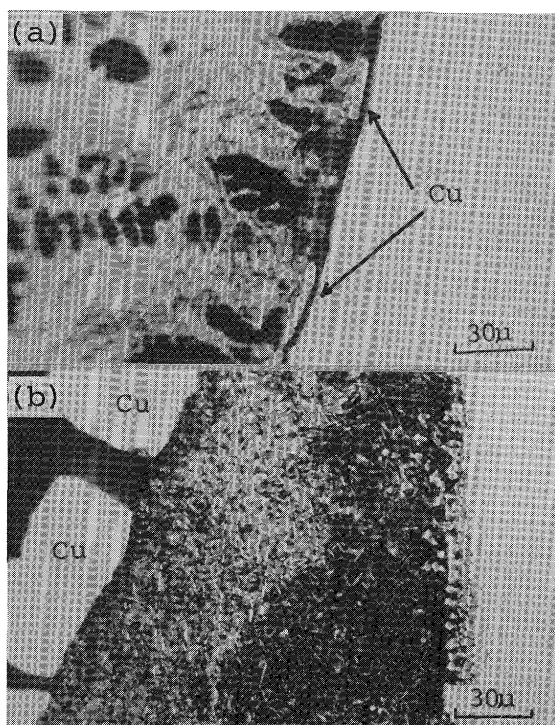
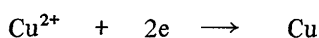


Fig. 9 Micrographs of deposited copper on filler alloy at brazed interface (a) and surface (b)

phase. Hence, the effective cathode site is believed to be  $\alpha_1$ -Ag phase.

The cathodic polarization curves of stainless steel is shown in Fig. 10. As well as the cathodic polarization curves of silver filler alloy, cathodic reaction increased with an increase in copper content of sodium chloride solution. Figure 11 shows the anodic polarization curves of stainless steel. Anodic reaction was also accelerated with increasing copper content in corrosive solutions, however, great differences were not recognized at about 0.4 V (S.C.E.). The results of polarization measurements indicate that the dissolution of stainless steel in test solution was mainly controlled by cathodic reaction, therefore, the interfacial corrosion of brazed stainless steel was enhanced by the increase in copper content in corrosive solutions. Polarization measurements and microscopic observation demonstrated that main cathodic reaction is the precipitation of copper from corrosive solution.



Anodic reaction is the dissolution of copper, zinc, cadmium from filler alloys, iron, chromium, nickel and other constituents from stainless steels. Copper has been shown to dissolve as cuprous ion<sup>6)</sup>.

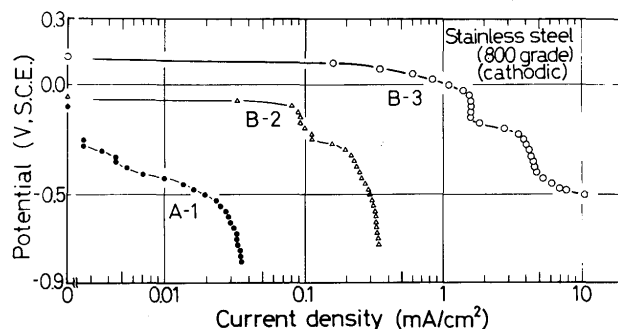


Fig. 10 Cathodic polarization curves of SUS 304

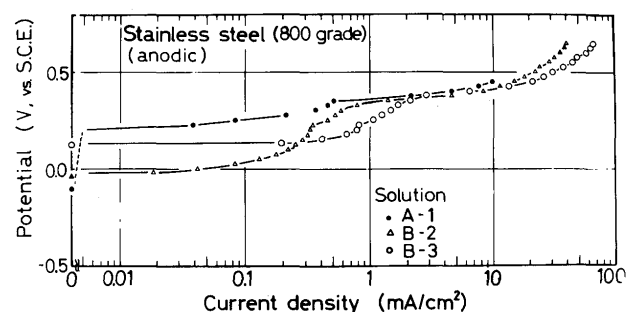
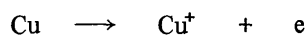


Fig. 11 Anodic polarization curves of SUS 304



A part of the cuprous ion might form  $\text{CuCl}$ . In fact, Pourbaix's diagram on  $\text{Cu}-\text{Cl}-\text{H}_2\text{O}$  system<sup>7)</sup> shows that  $\text{CuCl}$  is stable under the experimental conditions ( $\text{pH} \approx 4$ ,  $\text{CCl}^- \approx 0.1$ , electrode potential = 0 ~ 50 mV, S.C.E.).

#### 4. Discussions

The interfacial corrosion has sometimes made failure of the brazed joints during commercial use in moist atmosphere. The interfacial corrosion occurred at stainless steel side increased as the copper content in corrosive solutions was increased. The anodic dissolution of stainless steel was found to be controlled by the cathodic reaction.

The following descriptions deals with the mechanism of interfacial corrosion.

The brazing flux should exert an influence on the corrosion resistance of stainless steel at brazed interface, because one of the roles of brazing flux is removal of surface oxide films. The surface of stainless steel was

protected from corrosion by the passive films. For the sake of removal of this stable passive films, the brazing flux for stainless steel is consisted of some chlorides and halides. These aggressive chemical reagents have made the brazing of stainless steel possible. The effect of brazing flux on polarization characteristics of stainless steel was investigated to discuss the role of brazing flux for interfacial corrosion.

The surface of the stainless steel was covered with flux and heated at 830°C for 1 min and then air cooled. The stainless steel was rinsed in warm water to remove residual flux. A series of this treatment is called flux treatment. The cathodic polarization curves of flux treated surface was not so different from that of the emery polished surface. But the anodic reaction was accelerated by flux treatment as the change of current density per unit potential increased as shown in Fig. 12. The figure also shows that the electrode potential of flux treated specimens shifted toward base direction. From the results, the interfacial polarization curves could be schematically illustrated in Fig. 13. Corrosion potential and corrosion current are defined by the degree of anodic polarization. The flux treatment increased the corrosion current and decreased the corrosion potential. The flux treated surface was exposed in air for several hours before polarization test. The oxide film on flux treated surface grew during exposure in air. Under consideration of the growth of oxide film, the stainless steel at brazed interface which is suffered flux treatment and not reoxidized should easily dissolve anodically as compared with the results indicated in Figs. 12 and 13. The metallurgical characteristics of flux treated area was not clear because the layer is narrow, however, the brazing flux was considered to be a cause of the interfacial corrosion by electrochemical measurements.

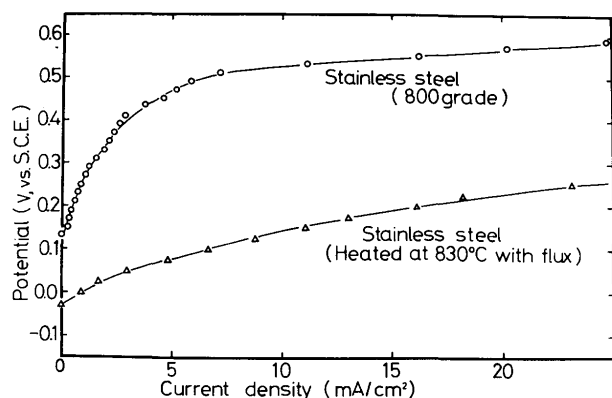


Fig. 12 Anodic polarization curves of SUS 304 of emery polished and treated with flux

Figure 14 shows the relation between the interfacial corrosion length (penetration length) and immersion time for BAg-1a and BAg-3 brazed stainless steel specimens. The dotted line in the figure shows that the interfacial corrosion proceeded through the whole interface of specimen. The penetration length increased parabolically with immersion time. The penetration length of BAg-3 brazed specimen was shorter than that of BAg-1a. The length of BAg-4 brazed specimen was also shorter than that of BAg-5. Nickel addition to filler alloy is thought to be effective on the improvement of interfacial corrosion resistance. One of the effect of nickel addition against the interfacial

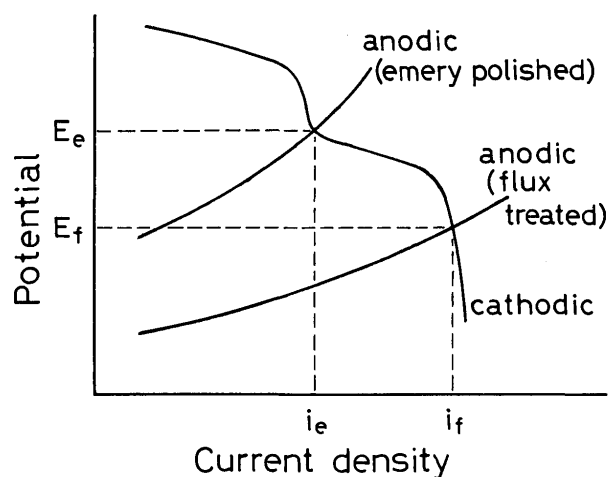


Fig. 13 Schematic illustration of internal polarization curves

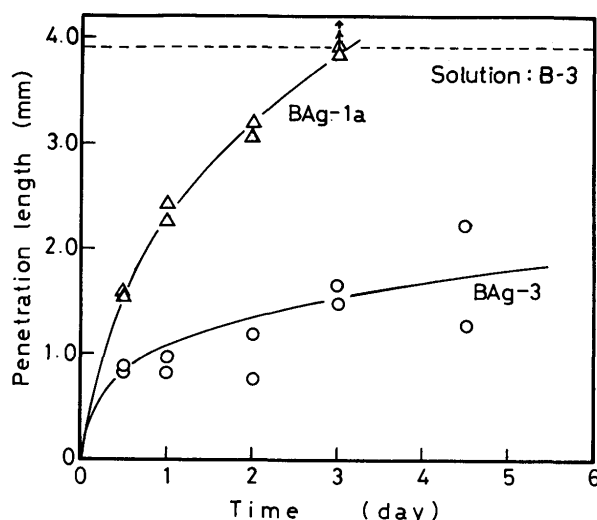


Fig. 14 Relations between interfacial penetration length and immersion time of BAg brazed stainless steel in B-3

corrosion is formation of nickel containing  $\alpha$ -Cu phase along brazed interface<sup>8)</sup>. The crystalization of nickel containing  $\alpha$ -Cu phase prevented the preferential dissolution of nickel from stainless steel. The dissolution of nickel from stainless steel formed nickel depleted zone in stainless steel at brazed interface. Nickel depleted zone might be inferior to the bulk alloy in corrosion resistance. The formation of nickel depleted zone in the specimen brazed with nickel free silver filler alloy might decrease the interfacial corrosion resistance. The formation process of nickel depleted zone in the case of BAg-5 brazed specimen and the formation of nickel containing  $\alpha$ -Cu phase in BAg-4 brazed specimens along brazed interface will be described in the other paper.

Figure 15 represents the schematic illustration of the cause of interfacial corrosion of silver brazed stainless steel. At brazed interface, the flux treated and nickel depleted zone was put between the silver filler alloy and stainless steel base alloy. As mentioned above, flux treated interface is easy to dissolve anodically. Therefore, this narrow region preferentially dissolved in corrosive solutions. Preferential dissolution of  $\alpha$ -Cu phase in brazed filler alloy shifted the corrosion potential toward noble direction during corrosion because the filler alloy enriched in silver owing to the dissolution of  $\alpha$ -Cu phase. This might accelerate the corrosion of neighbouring flux treated or nickel depleted zone.

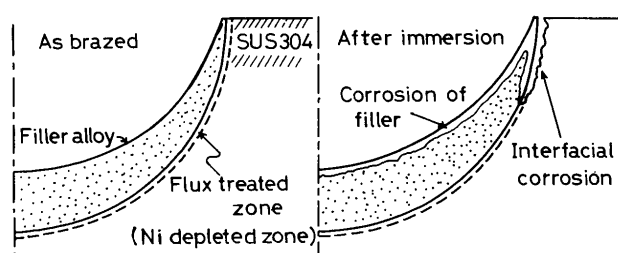


Fig. 15 Schematic illustration of interfacial corrosion of silver brazed stainless steel

## 5. Summary

The following conclusions were obtained by the corrosion test on silver brazed stainless steel in chloride solutions.

- (1) Stainless steel base plate and  $\alpha$ -Cu phase of silver filler alloy dissolved at brazed interface, and copper precipitated on silver filler alloy by cathodic reaction.
- (2) One of the cause of the dissolution of stainless steel at brazed interface was the removal of corrosion resistant passive films by brazing flux.
- (3) The pH of 0.4 mol/l NaCl aqueous solution changed with the added amount of  $\text{CuCl}_2 \cdot 2\text{H}_2\text{O}$ , however, there was no correlations between the pH change during corrosion test and corrosion parameters.
- (4) Dissolved copper from  $\alpha$ -Cu phase attached to the specimen surface as  $\text{CuCl}$ .

## Acknowledgement

The authors would like to thank Mr. C. Fujiwara for experimental works.

## References

- 1) S. Ekuni: "Corrosion Resistance of Brazing Filler Metals and Brazed Copper Joints", J. Japan Weld. Soc., **34** (1965), No.8, 785.
- 2) I. Kawakatsu: "Corrosion of BAg Brazed Joints in Stainless Steel", Weld. J., **52** (1973), No.6, 633-s.
- 3) G. H. Sistare, J. J. Halbig and L. H. Grenell: "Silver Brazing Alloys for Corrosion-Resistant Joints in Stainless Steels", Weld. J., **33** (1954), No.2, 137.
- 4) I. Okamoto, T. Takemoto and C. Fujiwara: "Corrosion Behaviour of Silver Brazed Stainless Steel in Chloride Solutions", J. Japan Weld. Soc., **48** (1979), No. 7, 510.
- 5) N. Ohtani: *Surface Engineering of Metals*, Nikkan Kogyo, (1963), 57.
- 6) U. Bertocci: *Electrochim Metal.*, **3** (1968), 275.
- 7) M. J. N. Pourbaix: *Thermodynamics of Dilute Aqueous Solutions*, Edward Arnold & Co., (1949), 53.
- 8) I. Okamoto and T. Takemoto: unpublished work